Appendix K.

Dewatering discharge modelling (RPS 2017d)

BAROSSA OFFSHORE DEVELOPMENT AREA
Dewatering Discharge Modelling

Prepared for ***ConocoPhillips Exploration Australia Pty Ltd***

12 OCTOBER 2017

Prepared by:

RPS

Suite E1, Level 4
140 Bundall Road
Bundall QLD 4217

T: +61 7 5574 1112
F: +61 8 9211 1122
E: Sasha.Zigic@rpsgroup.com.au

Client Manager: Dr Sasha Zigic
Report Number: MAQ0620J
Version / Date: Rev 2 | 12/10/2017

Prepared for:

CONOCOPHILLIPS EXPLORATION AUSTRALIA PTY LTD

Level 1,
53 Ord Street
West Perth WA 6005

T: +61 8 6363 3010

E: Tyron.Miley@contractor.conocophillips.com

Client Contact: Tyron Miley

Important Note

We have prepared this report for ConocoPhillips Exploration Australia Pty Ltd ("Client") for the specific purpose for which it is supplied ("Purpose"). This report is strictly limited to the Purpose including the facts and matters stated within it and is not to be used, directly or indirectly, for any other application, purpose, use or matter.

In preparing this report RPS has made certain assumptions. We have assumed that all information and documents provided to us by the Client or as a result of a specific request or enquiry were complete, accurate and up-to-date. Where we have obtained information from a government register or database, we have assumed that the information is accurate. Where an assumption has been made, we have not made any independent investigations with respect to the matters the subject of that assumption. As such we would not be aware of any reason if any of the assumptions were incorrect.

This report is presented without the assumption of a duty of care to any other person ("Third Party") (other than the Client). The report may not contain sufficient information for the purposes of a Third Party or for other uses. Without the prior written consent of RPS:

(a) this report may not be relied on by a Third Party; and

(b) RPS will not be liable to a Third Party for any loss, damage, liability or claim arising out of or incidental to a Third Party publishing, using or relying on the facts, content, opinions or subject matter contained in this report.

If a Third Party uses or relies on the facts, content, opinions or subject matter contained in this report with or without the consent of RPS, RPS disclaims all risk from any loss, damage, claim or liability arising directly or indirectly, and incurred by any third party, from the use of or reliance on this report.

In this note, a reference to loss and damage includes past and prospective economic loss, loss of profits, damage to property, injury to any person (including death) costs and expenses incurred in taking measures to prevent, mitigate or rectify any harm, loss of opportunity, legal costs, compensation, interest and any other direct, indirect, consequential or financial or other loss.

This report has been issued to the client under the agreed schedule and budgetary requirements and contains confidential information that is intended only for use by the client and is not for public circulation, publication, nor any third party use without the approval of the client.

Readers should understand that modelling is predictive in nature and while this report is based on information from sources that RPS considers reliable, the accuracy and completeness of said information cannot be guaranteed. Therefore, RPS, its directors, and employees accept no liability for the result of any action taken or not taken on the basis of the information given in this report, nor for any negligent misstatements, errors, and omissions. This report was compiled with consideration for the specified client's objectives, situation, and needs. Those acting upon such information without first consulting RPS, do so entirely at their own risk.

Document Status

Version	Purpose of Document	Original	Review	Review Date
Rev A	Preliminary results draft for internal review	Dr Ryan Dunn Dr Sasha Zigic	Dr Sasha Zigic	21/09/2017
Rev 0a	Preliminary results draft for client review		Dr Sasha Zigic	22/09/2017
Rev 1	Revision issued to client	Dr Ryan Dunn Dr Sasha Zigic	Dr Sasha Zigic	03/10/2017
Rev 2	Revision issued to client	Dr Sasha Zigic	Dr Sasha Zigic	12/10/2017

Approval for Issue

Name	Signature	Date
Dr Sasha Zigic		12/10/2017

Contents

Tables

Figures

Executive Summary

ConocoPhillips Australia Exploration Pty Ltd (ConocoPhillips), as proponent on behalf of the current co-venturers SK E&S Australia Pty Ltd and Santos Offshore Pty Ltd, is proposing to develop hydrocarbon resources in the Timor Sea into high quality products in a safe, reliable and environmentally responsible manner in the Barossa Area Development. The Barossa Area Development is located in Australian Commonwealth waters within the Bonaparte Basin, approximately 300 kilometres (km) north of Darwin, Northern Territory.

As the new gas export pipeline route is still subject to refinement, a corridor has been identified for the purposes of the early stage Offshore Project Proposal (OPP) to allow flexibility for placement pending further engineering and environmental investigations.

To inform the next submission of the Barossa OPP to the National Offshore Petroleum Safety and Environmental Management Authority (NOPSEMA), there is a need to undertake dewatering discharge modelling from the Barossa gas export pipeline. As the dewater will contain chemicals such as biocides and Monoethylene Glycol (MEG) at higher concentrations than the receiving water, ConocoPhillips have commissioned RPS to undertake a dispersion modelling study at the FPSO riser base manifold.

The modelling assessment was carried out based on an anticipated maximum discharge rate (and duration) and initial biocide concentrations:

- Discharge volume of 96,710 m^3 over a discharge period of 345.5 hours with initial biocide concentrations of 1,250 mg/L for Gluteraldehyde; 550 mg/L for THPS (Tetrakis (hydroxymethyl) phosphonium sulfate), and 550 mg/L for Hydrosure 0-3670R.

Results

The key findings are:

- The near-field results showed that due to the relative weak currents at the discharge depth (248.5 m), immediately upon discharge, the plume moved horizontally and maintained a low profile immediately above the seafloor.
- The near-field minimum dilution indicated that the average dilution of the dewatering discharge plume, 100 m from the release location, ranged from 1:32 to 1:58 under strong and weak currents, respectively
- The modelling indicates that the size of the area of potential effect ranged from 0.76 km^2 and 0.95 km^2, for Glutaraldehyde under transitional and winter conditions, respectively, and 0.54 km^2 and 0.63 km^2 for THPS or Hydrosure 0-3670R under transitional and winter conditions, respectively.
- Maximum distances required to achieve dilutions equivalent to 1 mg/L ranged from 1.21 km (winter conditions) – 1.27 km (summer) for Glutaraldehyde. For THPS or Hydrosure 0-3670R the required dilution would be achieved within a maximum distance of 0.84 km during winter conditions and up to 0.92 km under summer currents.
- The combined predicted area of coverage was 1.14 km^2 based on the use of Glutaraldehyde biocide and 0.75 km^2 for either THPS or Hydrosure 0-3670R biocide. The maximum distance predicted was 1.27 km based on the seasonally combined assessment.

1.0 Introduction

ConocoPhillips Australia Exploration Pty Ltd (ConocoPhillips), as proponent on behalf of the current co-venturers SK E&S Australia Pty Ltd and Santos Offshore Pty Ltd, is proposing to develop hydrocarbon resources in the Timor Sea into high quality products in a safe, reliable and environmentally responsible manner in the Barossa Area Development. The Barossa Area Development (herein referred to as the project) is located in Australian Commonwealth waters within the Bonaparte Basin, approximately 300 kilometres (km) north of Darwin, Northern Territory (NT; Figure 1.1).

The development concept includes a permanently moored floating, production, storage and offtake (FPSO) facility, subsea production system, supporting in-field subsea infrastructure in the Barossa Field (petroleum retention lease NT/RL5) and a subsea gas export pipeline. The FPSO facility will separate the natural gas and condensate extracted from the field with the condensate exported directly from the FPSO facility to offtake tankers in the Barossa offshore development area and the dry gas transported via a subsea gas export pipeline for onshore processing.

It is proposed that the new subsea gas export pipeline be connected to the existing Bayu-Undan to Darwin gas export pipeline which feeds the onshore Darwin Liquefied Natural Gas facility at Wickham Point, NT. This would allow transport of dry gas from the project to Darwin for liquefaction and export. Gas from the project would replace the existing supply from the Bayu-Undan Field following its anticipated depletion in 2022 (subject to appropriate commercial arrangements being put in place).

As the new gas export pipeline route is still subject to refinement, a corridor has been identified for the purposes of the early stage Offshore Project Proposal (OPP) to allow flexibility for placement pending further engineering and environmental investigations.

To inform an assessment of the potential impacts to the marine environment from dewatering of the flooding fluid from the new gas export pipeline, there is a need to undertake dewatering discharge modelling.

The flooding fluid to be dewatered will consist of filtered inhibited seawater containing residual chemicals, such as biocides and Monoethylene Glycol (MEG), corrosion inhibitor, scale inhibitor, dye and oxygen scavengers at higher concentrations than the receiving water. Consequently, ConocoPhillips have commissioned RPS to undertake a dispersion modelling study at the FPSO riser base manifold (Table 1.1 and Figure 1.1).

The principal aim of this study was to provide a preliminary quantification of potential effects from the release of chemicals within the dewatering plume discharge during commissioning activities for the project.

The potential area that may be influenced by the dewatering plume was assessed for three distinct seasons; (i) summer (December to the following February), (ii) the transitional periods (March and September to November) and (iii) winter (April to August). This approach assists with identifying the environmental values and sensitivities that would be at risk of exposure on a seasonal basis.

The closest environmental values and sensitivities to the modelled release location are submerged shoals and banks including Lynedoch Bank (64 km to the south-east), Evans Shoal (71 km to the west) and Tassie Shoal (82 km to the south-west).

Table 1.1 Barossa offshore development area dewatering plume dispersion modelling assessment.

Release Site	Latitude (S)	Longitude (E)	Water Depth (m)
Barossa offshore development area – FPSO riser base manifold	9° 50’ 5.0"	130° 14’ 30.5"	252

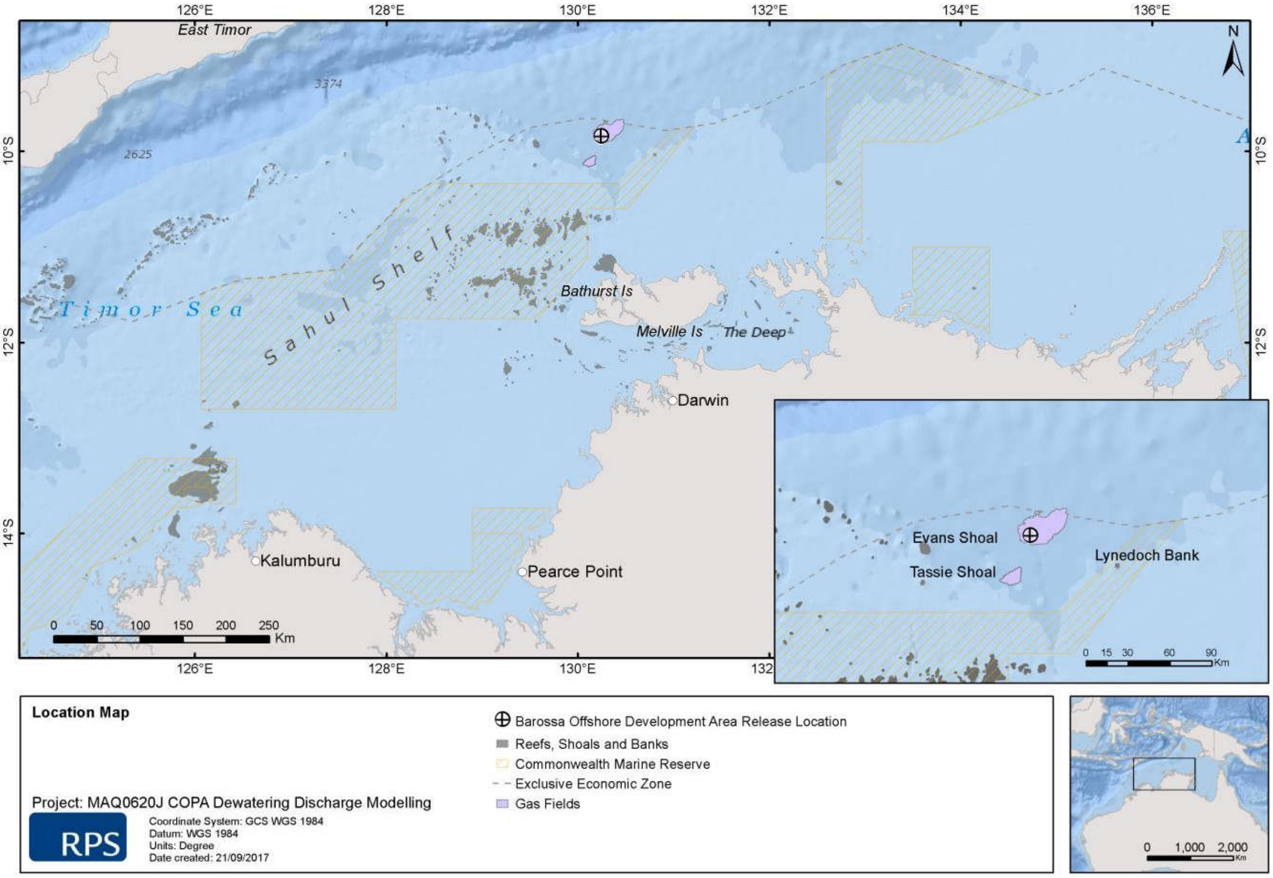

Figure 1.1 Map of the Barossa offshore development area dewatering plume study release location.

2.0 Dispersion Modelling

The physical mixing of the dewatering plume can be separated into two distinct zones: (a) near-field; and (b) far-field. The limits of the near-field zone is defined by the area where the levels of mixing and dilution are controlled by the plume's initial jet momentum and the buoyancy flux.

Therefore, to accurately determine the dilution of the discharge and the mixing zones, the effect of near-field dynamics was considered initially, followed by, an in conjunction with, the far-field modelling assessment. During the far-field phase, the plume is transported and mixed by the ambient currents.

Section 2.1 and Section 2.2 describe the near-field and far-field dispersion model setup and inputs, respectively.

2.1 Near-Field Model

2.1.1 Description

The near-field mixing of the dewatering discharge stream was predicted using the fully three-dimensional flow model, Updated Merge (UM3). The UM3 model is used for simulating single and multi-port submerged discharges and is part of the Visual Plumes suite of models maintained by the United States Environmental Protection Agency (Frick et al. 2003).

The UM3 model has been extensively tested for various discharges and found to predict the observed dilutions more accurately (Roberts and Tian 2004) than other near-field models (e.g. RSB or CORMIX).

In this Lagrangian model, the equations for conservation of mass, momentum, and energy are solved at each time-step, giving the dilution along the plume trajectory. To determine the growth of each element, UM3 uses the shear (or Taylor) entrainment hypothesis and the projected-area-entrainment hypothesis. Model output consists of plume characteristics, including dilution, rise-rate, width, centreline height and diameter of the plume. Dilution is reported as the "effective dilution", which is the ratio of the initial concentration to the concentration of the plume at a given point, following Baumgartner et al. (1994).

2.1.2 Model setup

The dewatering discharge characteristics are summarised in Table 2.1. The dewatering discharge was modelled 3.5 m above the seafloor (water depth 252 m) from a single outlet. The temperature and salinity of the discharged plume was anticipated to be that of ambient waters. As the type of biocide to be used for the project is yet to be selected, three biocides were modelled; Gluteraldehyde, Tetrakis (hydroxymethyl) phosphonium sulfate (THPS) and Hydrosure 0-3670R. The initial biocide concentrations were assumed at 1,250 mg/L for Gluteraldehyde, 550 mg/L for THPS, and 550 mg/L for Hydrosure 0-3670R.

The discharge rate is anticipated to range between 280 m^3/h to 810 m^3/h for a 26 inch diameter pipe and 320 m^3/h to 950 m^3/h for a 28 inch pipe based on a PIG speed of 0.25 m/s to 0.75 m/s. Additionally, maximum durations are anticipated to range from 345.4 hours for the 280 m^3/h discharge rate to 85.9 hours for the 950 m^3/h discharge rate. A maximum discharge volume of 96,710 m^3 over a discharge period of 345.5 hour was modelled. This scenario was modelled as it is considered the most conservative in terms of representing the potential maximum extent of the dewatering plume discharge.

Additional input data used to setup the near-field model included a range of current speeds, water temperature and salinity. The salinity and temperature data was sourced from a measured dataset at depth of 253 m nearby the modelled discharge location collected by Fugro (2015) as part of the Barossa marine studies program. Table 2.2 presents the measured water temperature and salinity data used to describe the ambient water column conditions.

Table 2.3 presents the 5th, 50th and 95th percentiles of current speeds, which reflect potentially contrasting dilution and advection cases:

- 5th percentile current speed: relative weak currents,
- 50th percentile (median): relative medium current speed, and
- 95th percentile current speed: relative strong currents.

The 5th percentile, 50th percentile (median) and 95th percentile values are referenced as weak, medium and strong current speeds, respectively.

Table 2.1 Dewatering plume discharge and pipe configuration characteristics summary.

Parameter	Value/design
Maximum discharge volume	96,710 m^3
Maximum flow rate	280 m^3/h
Outlet pipe internal diameter	26 inch
Pipe orientation	Horizontal
Depth of pipe below sea surface	248.5 m
Height of pipe above seafloor	3.5 m
Discharge salinity	Based on ambient conditions (near the seabed) 33.9 practical salinity units (psu) (summer conditions) 33.9 psu (transitional conditions) 33.9 psu (winter conditions)
Discharge water temperature	Based on ambient conditions (near the seabed) 12.8 °C (summer conditions) 12.8 °C (transitional conditions) 12.7 °C (winter conditions)
Initial biocide dosing concentrations	1,250 mg/L – Gluteraldehyde 550 mg/L – THPS 550 mg/L – Hydrosure 0-3670R

Table 2.2 Water temperature and salinity model inputs.

Parameter	Season		
	Summer	Transitional	Winter
Ambient minimum water temperature at 252 m water depth (°C)	12.8	12.8	12.7
Ambient mean salinity (Practical Salinity Units at 252 m water depth (PSU)	33.9	33.9	33.9

Table 2.3 Seasonal ambient percentile current speeds, strength and predominant direction as a function of water depth at the release location.

Depth below the water surface (m)	Parameter	Reporting current strength	Season					
			Summer		Transitional		Winter	
			Speed (m/s)	Predominant direction	Speed (m/s)	Predominant direction	Speed (m/s)	Predominant direction
230	5th percentile	Weak	0.01	North-northwest	0.01	North-northwest	0.01	North-northwest
	50th percentile	Medium	0.03		0.03		0.03	
	95th percentile	Strong	0.08		0.07		0.07	
240	5th percentile	Weak	0.01	North-northwest	0.01	North-northwest	0.01	North-northwest
	50th percentile	Medium	0.03		0.03		0.03	
	95th percentile	Strong	0.08		0.07		0.07	
250	5th percentile	Weak	0.01	North-northwest	0.01	North-northwest	0.01	North-northwest
	50th percentile	Medium	0.03		0.03		0.03	
	95th percentile	Strong	0.08		0.07		0.07	

2.2 Far-field Model

2.2.1 Description

The far-field modelling expands on the near-field model predictions as it also takes into account the time-varying nature of currents, together with the potential for recirculation of the plume back to the release location. In the latter case near-field concentrations can be increased due to the discharge plume mixing with the remnant plume from an earlier time.

The three-dimensional plume behaviour model, MUDMAP, was used to simulate the far-field mixing and dispersion of biocide concentrations within the discharged dewatering plume. MUDMAP is an industry standard computerised modelling system, which has been applied throughout the world to predict the dispersion of sediment (cuttings and muds) and liquid (produced water) discharges since 1994 (Spaulding, 1994). The model is a development of the Offshore Operators Committee (OOC) model and like the OOC model calculates the fates of discharges through three known distinct integrated stages (Koh and Chang 1973; Khondaker 2000; Brandsma and Sauer 1983a, 1983b).

The dewatering release is represented by placing a fixed number of “particles” at the release location at each model time-step. These particles are moved on each subsequent time-step according to the horizontal and vertical components from the hydrodynamic model. The plume spread is dependent on the horizontal and vertical mixing coefficients.

The MUDMAP system is based on a conservative tracer (no reaction or decay) to examine the mixing and dilution of discharge plumes. The concentration distribution of the constituent in water is estimated using a counting grid. The number of particles in a grid square over a depth interval from the water surface down to a specified depth is counted, giving the mass of the constituent in a known volume, and therefore concentration.

The system has been validated and applied for discharge operations in Australian waters (e.g. Burns et al. 1999; King and McAllister 1997, 1998).

2.2.2 Model setup

The MUDMAP model simulated the discharge into a time-varying current field with the initial dilution set by the near-field results described in Section 2.1.

The dewatering discharge rates were modelled as a constant discharge for each month during 2010, 2012 and 2014. Once the results were complete, they were reported on a combined seasonal basis: (i) summer (December to the following February); (ii) the transitional (March, April, September to November) and (iii) winter (May to August).

MUDMAP uses a three-dimensional grid to represent the water depth and bathymetric profiles of the study area. Due to the discharge conditions, mixing, current speeds and small-scale influences of the discharge, it was necessary to use a very fine grid with a resolution of 2 m x 2 m to track the movement and fate of the plume above the seafloor. The extent of the grid region measured 2 km (longitude or x-axis) x 2 km (latitude or y-axis). It is important to note, that the 2 m grid cell sizes were selected following extensive sensitivity testing in order to achieve similar dilution rates predicted during the near-field modelling.

Table 2.4 presents a summary of the far-field model parameters used to simulate the dewatering plume discharges during the three seasons assessed.

Spatially constant, conservative horizontal and vertical dispersion coefficients were used to control the exchange of the dewatering plume in the horizontal and vertical directions respectively. The coefficients were selected following sensitivity testing in order to recreate similar plume characteristics and dilutions predicted during the near-field modelling.

Table 2.4 Summary of the far-field dewatering model inputs.

Parameter	Value/design
Years simulated	2010 (La Niña conditions) 2012 (neutral/mixed) 2014 (El Niño conditions)
Seasons (months simulated and reported)	Summer (December, January, February) Transitional periods (March, April, September to November) Winter (May to August)
Commencement date of each modelled calendar month	1st day of each calendar month 15th day of each calendar month
Total months modelled	36
Total runs analysed	72
Flow rate	280 m^3/h
Discharge type	Continuous
Discharge duration	345.4 h
Model duration	417.4 h
Dewatering discharge temperature	Based on ambient conditions (near the seabed) 12.8 °C (summer conditions) 12.8 °C (transitional conditions) 12.7 °C (winter conditions)
Dewatering discharge salinity	Based on ambient conditions (near the seabed) 33.9 psu (summer conditions) 33.9 psu (transitional conditions) 33.9 psu (winter conditions)
Initial biocide dosing concentrations	1,250 mg/L – Gluteraldehyde 550 mg/L – THPS 550 mg/L – Hydrosure 0-3670R

2.3 Interannual Variability

The region is strongly affected by the strength of the Indonesian Throughflow, which fluctuates from one year to the next due to the exchange between the Pacific and Indian Oceans. Therefore, in order to examine the potential range of variability, the Southern Oscillation Index (SOI) data sourced from the Australian Bureau of Meteorology was used to identify interannual trends for the 10 year period 2005 to 2014. The SOI broadly defines neutral, El Niño (sustained negative values of the SOI below −8 often indicate El Niño episodes) and La Niña (sustained positive values of the SOI above +8 are typical of La Niña episodes) conditions based on differences in the surface air-pressure between Tahiti on the eastern side of the Pacific Ocean and Darwin (Australia), on the western side (Rasmusson and Wallace 1983, Philander 1990). El Niño episodes are usually accompanied by sustained warming of the central and eastern tropical Pacific Ocean and a decrease in the strength of the Pacific trade winds. La Niña episodes are usually associated with converse trends (i.e. increase in strength of the Pacific trade winds).

Figure 2.1 shows the SOI monthly values for the period 2005–2014 at the proposed release location. Each current rose diagram provides an understanding of the speed, frequency and direction of currents, over the given year:

Based on the combination of the SOI assessment and surface ocean currents, 2010 was selected as a representative La Niña year, 2012 was selected as a representative neutral year, and 2014 was selected as an El Niño year.

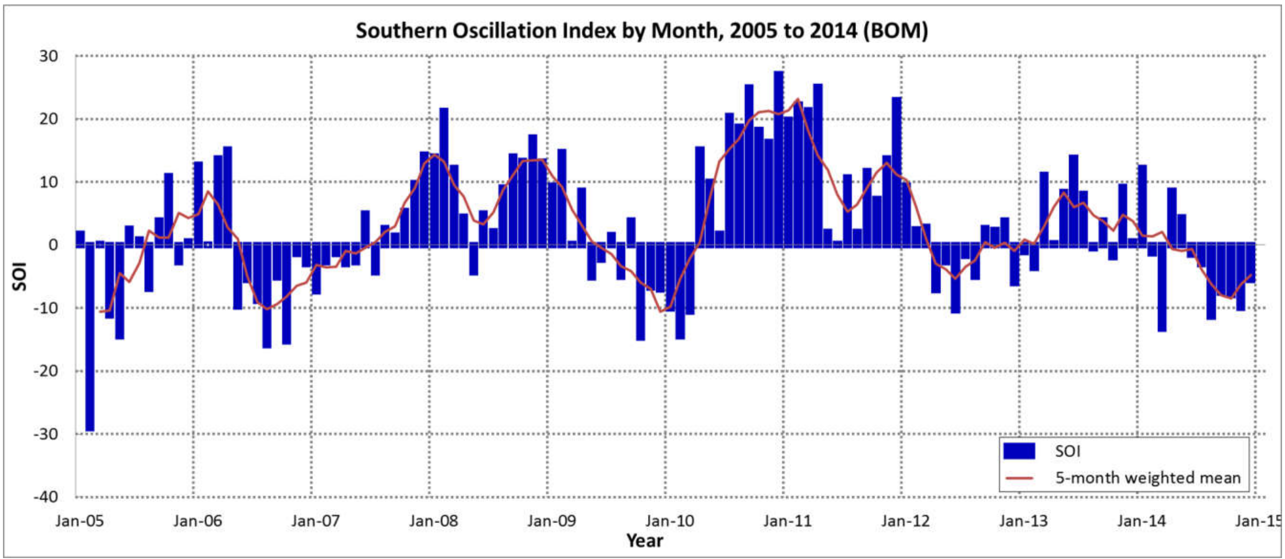

Figure 2.1 Monthly values of the SOI 2005-2014. Sustained positive values indicate La Niña conditions, while sustained negative values indicate El Niño conditions (Data sourced from Australian Bureau of Meteorology 2015).

2.4 Development of Regional Current Data

2.4.1 Tidal currents

The effects of tides were generated using RPS's advanced ocean/coastal model, HYDROMAP. The HYDROMAP model has been thoroughly tested and verified through field measurements throughout the world over since 1984 (Isaji and Spaulding, 1984; Isaji et al., 2001; Zigic et al., 2003). In addition, HYDROMAP tidal current data has been used as input to forecast (in the future) and hindcast (in the past) hydrocarbon spills in Australian waters and forms part of the Australian National Oil Spill Emergency Response System operated by the Australian Maritime Safety Authority (AMSA).

The numerical solution methodology follows that of Davies (1977a and 1977b) with further developments for model efficiency by Owen (1980) and Gordon (1982). A more detailed presentation of the model can be found in Isaji and Spaulding (1984) and Isaji et al. (2001).

The ocean boundary data for the regional model was obtained from satellite measured altimetry data (TOPEX/Poseidon 7.2) which provided estimates of the eight dominant tidal constituents at a horizontal scale of approximately 0.25 degrees. Using the tidal data, surface heights were firstly calculated along the open boundaries, at each time step in the model.

The Topex-Poseidon satellite data is produced and quality controlled by the National Aeronautics and Space Administration (NASA). The satellites, equipped with two highly accurate altimeters that are capable of taking sea level measurements to an accuracy of less than 5 cm, measured oceanic surface elevations (and the resultant tides) for over 13 years (1992–2005; see Fu et al., 1994; NASA Propulsion Laboratory 2013a; 2013b). In total, these satellites carried out 62,000 orbits of the planet. The Topex-Poseidon tidal data has been widely used amongst the oceanographic community, being included in more than 2,100 research publications (e.g. Andersen 1995, Ludicone et al. 1998, Matsumoto et al. 2000, Kostianoy et al. 2003, Yaremchuk and Tangdong 2004, Qiu and Chen 2010). As such the Topex/Poseidon tidal data is considered accurate for this study.

2.4.2 Ocean currents

Data describing the flow of ocean currents was obtained from the Hybrid Coordinate Ocean Model (HYCOM) (see Chassignet et al. 2007, 2009), which is operated by the HYCOM Consortium, sponsored by the Global Ocean Data Assimilation Experiment (GODAE). HYCOM is a data-assimilative, three-dimensional ocean model that is run as a hindcast, assimilating time-varying observations of sea surface height, sea surface temperature and in-situ temperature and salinity measurements (Chassignet et al. 2009). The HYCOM predictions for drift currents are produced at a horizontal spatial resolution of approximately 8.25 km (1/12th of a degree) over the region, at a frequency of once per day. HYCOM uses isopycnal layers in the open, stratified ocean, but uses the layered continuity equation to make a dynamically smooth transition to a terrain following coordinate in shallow coastal regions, and to z–level coordinates in the mixed layer and/or unstratified seas.

For this modelling study, the HYCOM hindcast currents were obtained for the years 2010 to 2014 (inclusive). The data shows that the bottom speeds and directions varied minimally between seasons.

2.5 Environmental reporting criteria

The flooding fluid discharged during dewatering will contain the following chemical additives:

- Biocide to prevent biological corrosion and
- MEG, a hydrate inhibitor (antifreeze)

Three types of biocides are being considered and their concentrations vary:

- Glutaraldehyde – 1,250 ppm
- THPS – 550 ppm
- Hydrosure 0-3670R – 550 ppm

The biocide threshold concentration/trigger value used as part of this study was 1 ppm (equivalent to 1 mg/L) and is based on the published acute toxicity test data presented by Chevron (2015). This equates to dilutions of:

- Gluteraldehyde – 1:1,250
- THPS – 1:550
- Hydrosure 0-3670R –1:550

Studies have previously been conducted to assess the biodegradation of MEG in the marine environment. The reported toxicity is 10,000 ppm (ppm is equivalent to mg/L) (48 hr LC_{50} for algae and *Daphnia* (planktonic crustacean genus); 96 hr LC_{50} for fish species). MEG is generally not considered harmful or toxic to aquatic organisms and is readily biodegradable (G-Biosciences 2017).

As such, the biocide was identified as having the highest toxicity and was used to determine the maximum extent associated with the discharge.

3.0 Modelling Results

3.1 Near-field Modelling

The near-field results showed that due to the relative weak currents at the discharge depth (248.5 m), in concert with the lack of density and temperature differences between the dewatering plume and receiving environment, which would otherwise promote plume mixing and thus dilution, the plume maintained a low profile immediately above the seafloor, whilst drifting horizontally from the release location. As the plume continued to mix with the ambient bottom waters the dilution of the plume increased with increasing distance from the release location. Table 3.1 shows the predicted plume characteristics based upon the varying current speeds (i.e. 5th, 50th and 95th percentile current speeds). For all seasons, the primary factor influencing dilution of the dewatering plume was the strength of the ambient currents. The relatively stronger currents retarded the mixing of the plume profile resulting from a decreased plume diameter, whilst the weaker ambient currents allowed for a greater diameter, corresponding to greater dilution. For example, during stronger currents the plume diameter ranged from 6.1 m and 20.4 m, 100 m from the release location, under strong and weak currents, respectively. The plume was predicted to interact with the seafloor under all ambient conditions.

The minimum dilution, based on the centreline dilution value of the plume 100 m from the release location, ranged between 1:9 and 1:20 under strong and weak currents, respectively, whilst the average dilution of the plume, 100 m from the release location, ranged from 1:32 to 1:58 under strong and weak currents, respectively (see Figure 3.1 to Figure 3.3).

Due to the limited seasonal variability of ambient water column conditions near the seabed the seasonal near-field modelling results demonstrated no discernible difference in the plume behaviour between summer, winter and transitional seasons.

Note that these predictions rely on the persistence of current speed and direction over time and does not account for the build-up of the plume.

Table 3.1 Predicted plume characteristics at 100 m from release location based on 280 m^3/h discharge for each season and current speed.

Season	Current speed (m/s)	Dilution of the plume (1:x)		Plume diameter (m) (near the seabed)
		Minimum (based on centreline of plume)	Average	
Summer	Weak (0.01)	20	58	20.4
	Medium (0.03)	12	43	9.8
	Strong (0.08)	9	32	6.1
Transitional	Weak (0.01)	20	58	20.4
	Medium (0.03)	12	43	9.8
	Strong (0.07)	9	32	6.1
Winter	Weak (0.01)	20	58	20.3
	Medium (0.03)	12	43	9.8
	Strong (0.07)	9	32	6.1

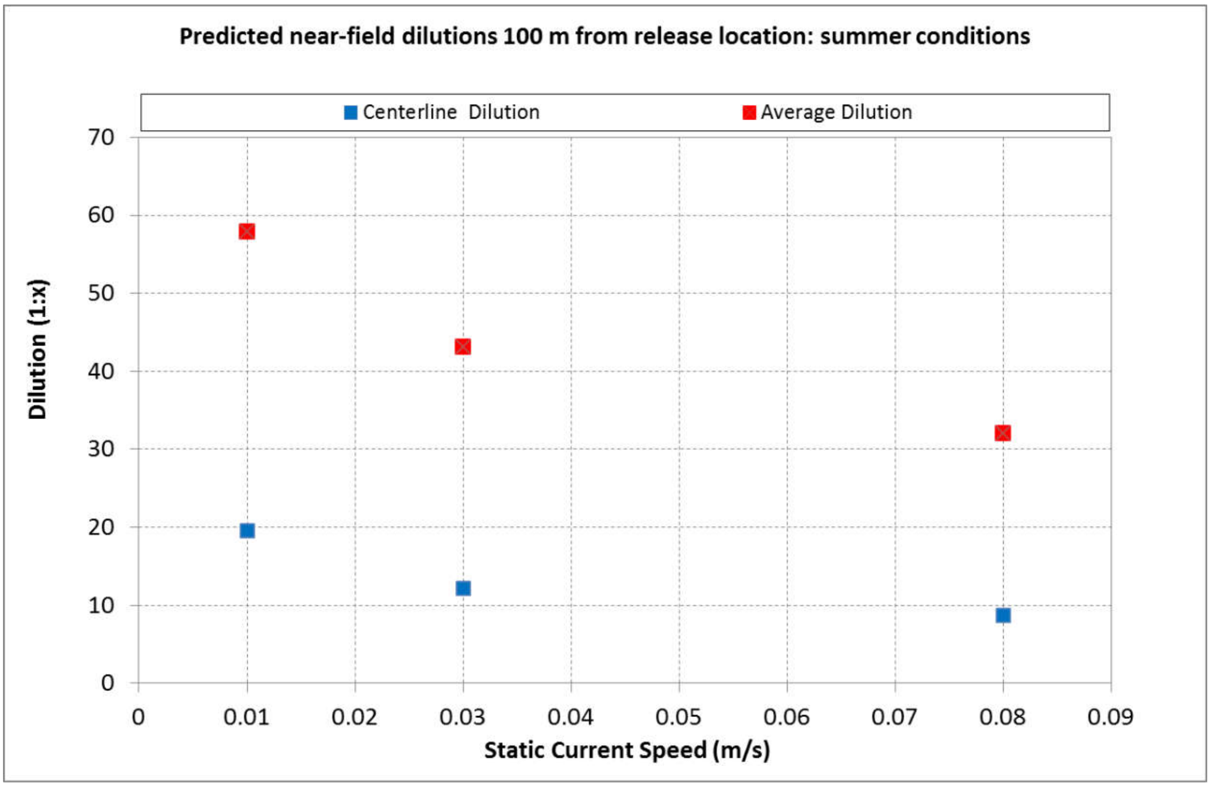

Figure 3.1 Near-field dilution results at 100 m from release location based on 280 m^3/h discharge during summer conditions and current speed.

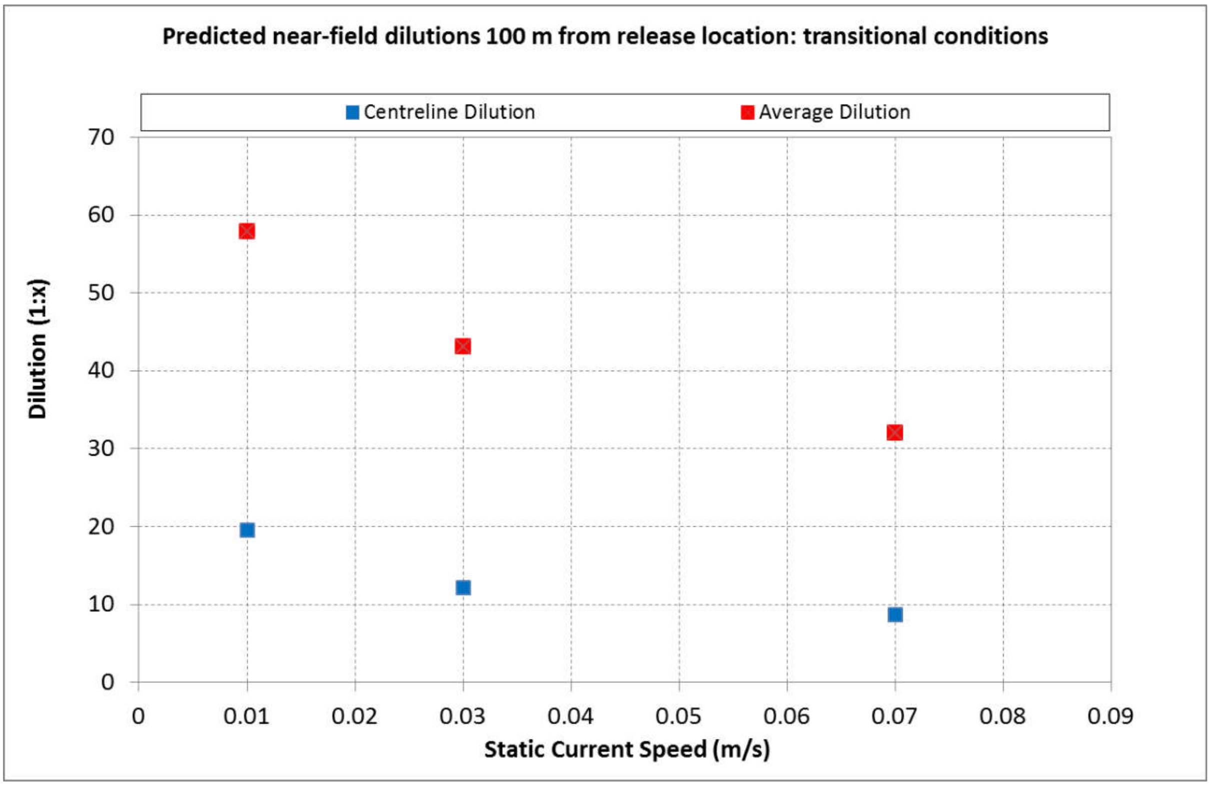

Figure 3.2 Near-field dilution results at 100 m from release location based on 280 m^3/h discharge during transitional conditions and current speed.

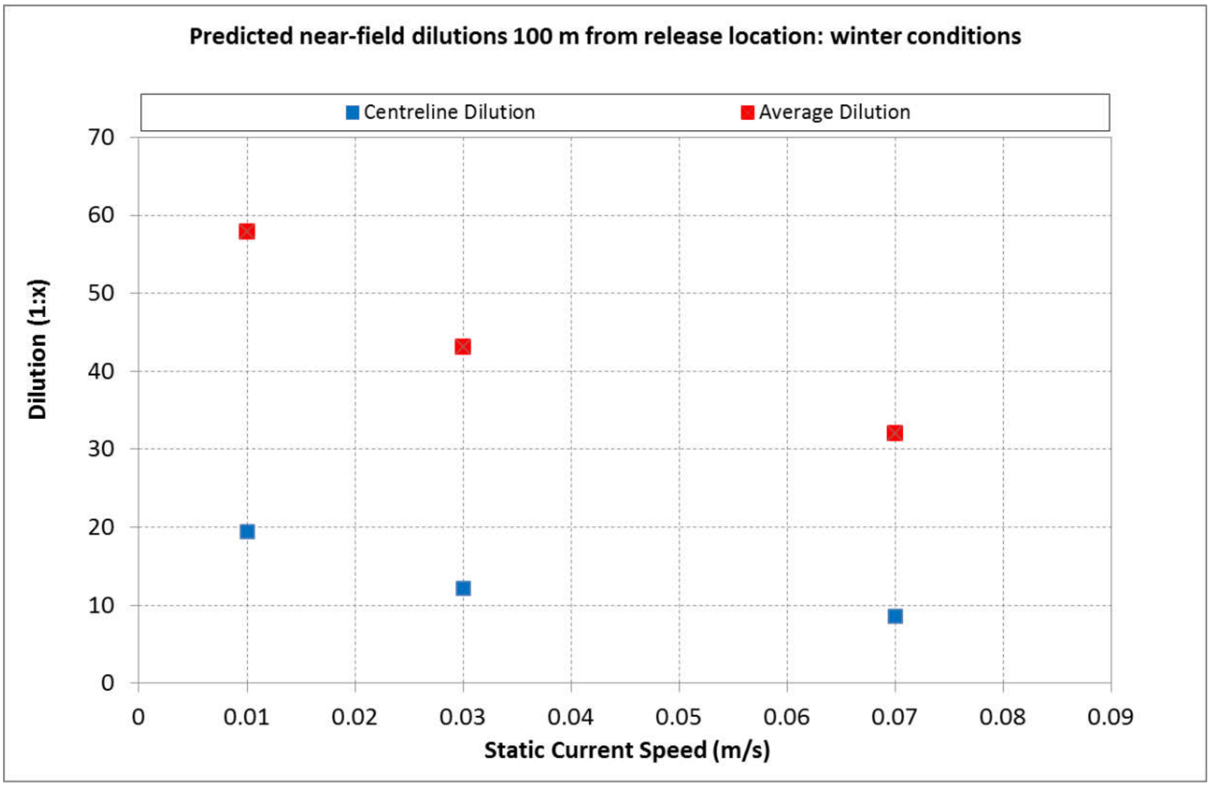

Figure 3.3 Near-field dilution results at 100 m from release location based on 280 m^3/h discharge during winter conditions and current speed.

3.2 Far-Field Modelling

3.2.1 General observations

Figure 3.4 and Figure 3.5 show example model screenshots of predicted dilutions (equivalent concentrations) for biocide within the dewatering plume, every 4 hours from 5 pm 17th December 2014 to 5 am 18th December 2014.

The images have been included to illustrate the movement and dilution (and in turn concentrations) of the plume within an example time period as a result of time-varying current directions and speeds. The cross sections illustrated the plume moving horizontally and maintaining a low profile immediately above the seafloor.

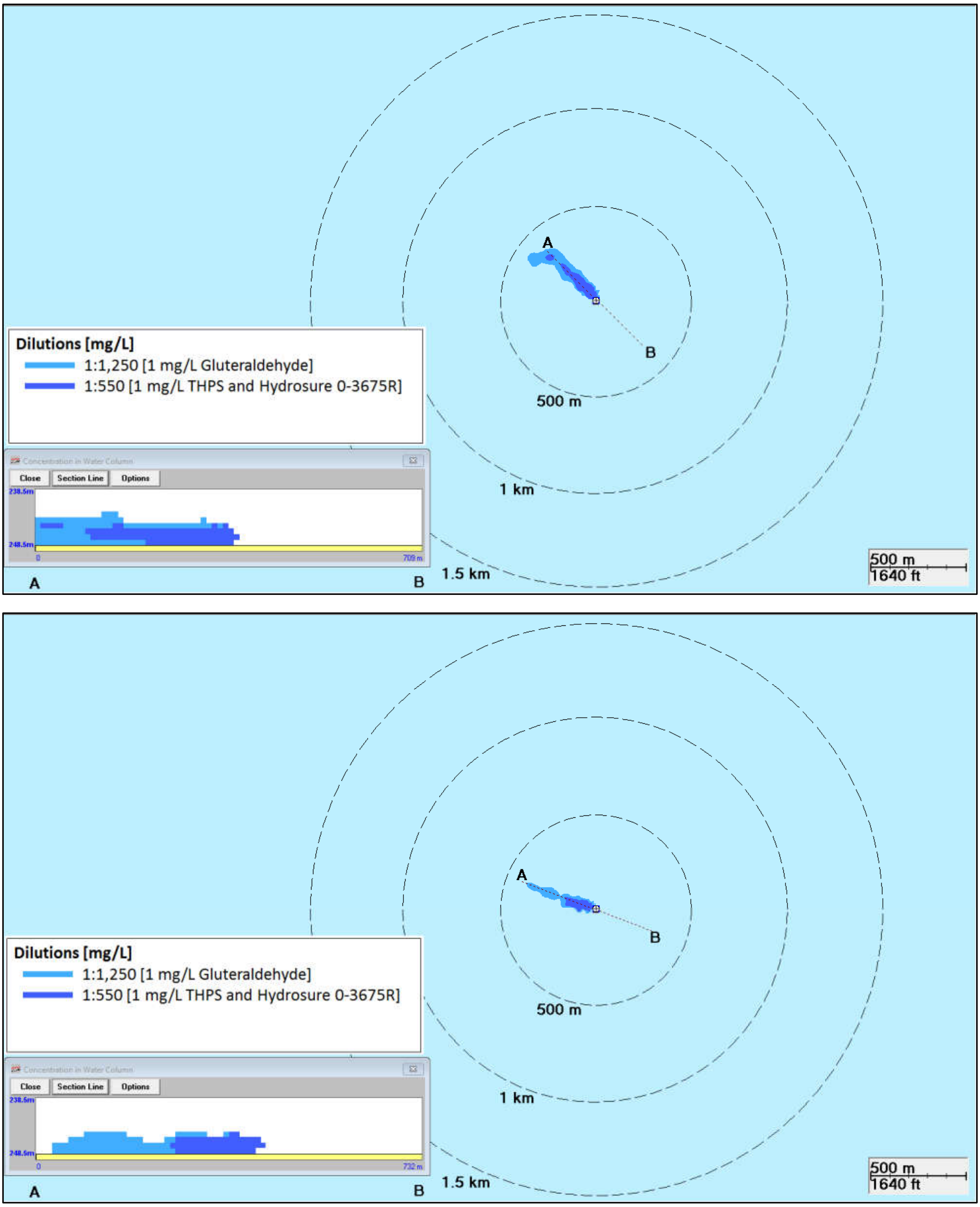

Figure 3.4 Example screenshots of the predicted biocide dilutions (and equivalent concentration, mg/L) 5 pm 17th December 2014 (upper figure) and 9 pm 17th December 2014 (lower figure). Figure insets illustrate zoomed-in cross water profile of 10 m depth from seafloor.

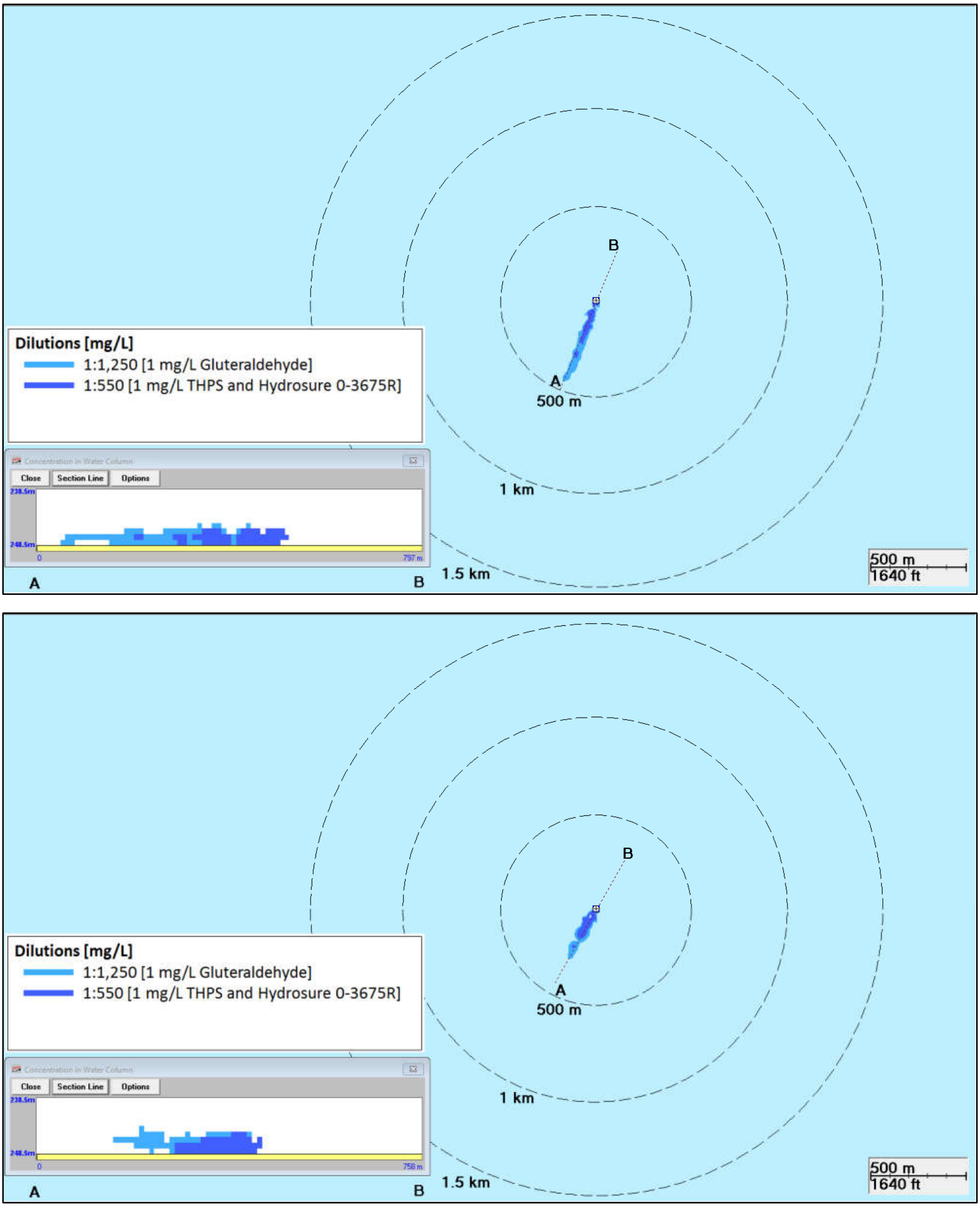

Figure 3.5 Example screenshots of the predicted biocide dilutions (and equivalent concentration, mg/L) 1 am 18th December 2014 (upper figure) and 5 am 18th December 2014 (lower figure). Figure insets illustrate zoomed-in cross water profile of 10 m depth from seafloor.

3.2.2 Seasonal analysis

The 60 minute model outputs for each month (including the two commencement times) from each of the three years (2010, 2012 and 2014) were combined and analysed according to the respective season (i.e. summer – December, January, February; transitional periods – March, April and September to November; and winter – May to August). This approach assists with identifying the potential for exposure on a seasonal basis, based on far-field variations in ambient current speeds and directions.

Table 3.2 provides a summary of the area of coverage and maximum distance predicted to achieve dilutions resulting in biocide concentrations of 1 mg/L.

The modelling indicates that the size of the area of potential effect ranged from 0.76 km^2 and 0.95 km^2, for Glutaraldehyde under transitional and winter conditions, respectively, and 0.54 km^2 and 0.63 km^2 for THPS or Hydrosure 0-3670R under transitional and winter conditions, respectively. Maximum distances required to achieve dilutions equivalent to 1 mg/L ranged from 1.21 km (winter conditions) – 1.27 km (summer) for Glutaraldehyde. For THPS or Hydrosure 0-3670R the required dilution would be achieved within a maximum distance of 0.84 km during winter conditions and up to 0.92 km under summer currents (Table 3.2).

Figure 3.6 to Figure 3.8 show the extent to achieve dilutions resulting in biocide concentrations of 1 mg/L under summer, transitional and winter conditions. Note that the images represent the lowest predicted dilution at any given time-step through the water column and do not take into account frequency or duration.

Table 3.2 Summary of the area of coverage and maximum distance to achieve dilutions resulting in biocide concentrations of 1 mg/L during each season.

Biocide	Initial biocide concentration (mg/L)	Dilution required to achieve biocide concentrations of 1 mg/L	Season	Area of coverage (km^2)	Maximum distance (km) from the release location
Gluteraldehyde	1,250	1:1,250	Summer	0.82	1.27
			Transitional	0.76	1.26
			Winter	0.95	1.21
THPS or Hydrosure 0-3670R	550	1:550	Summer	0.55	0.92
			Transitional	0.54	0.86
			Winter	0.63	0.84

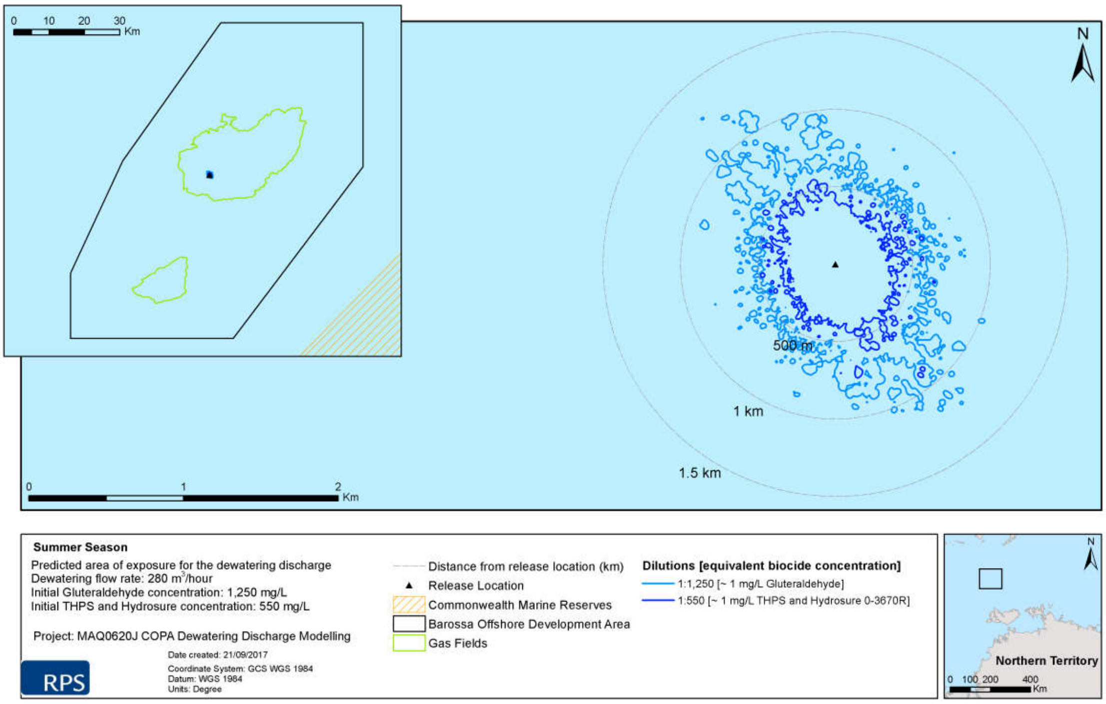

Figure 3.6 Predicted extent to achieve dilutions resulting in biocide concentrations of 1 mg/L under summer (December to the following February) conditions for the 280 m^3/h flow rate (96,710 m^3 total discharge).

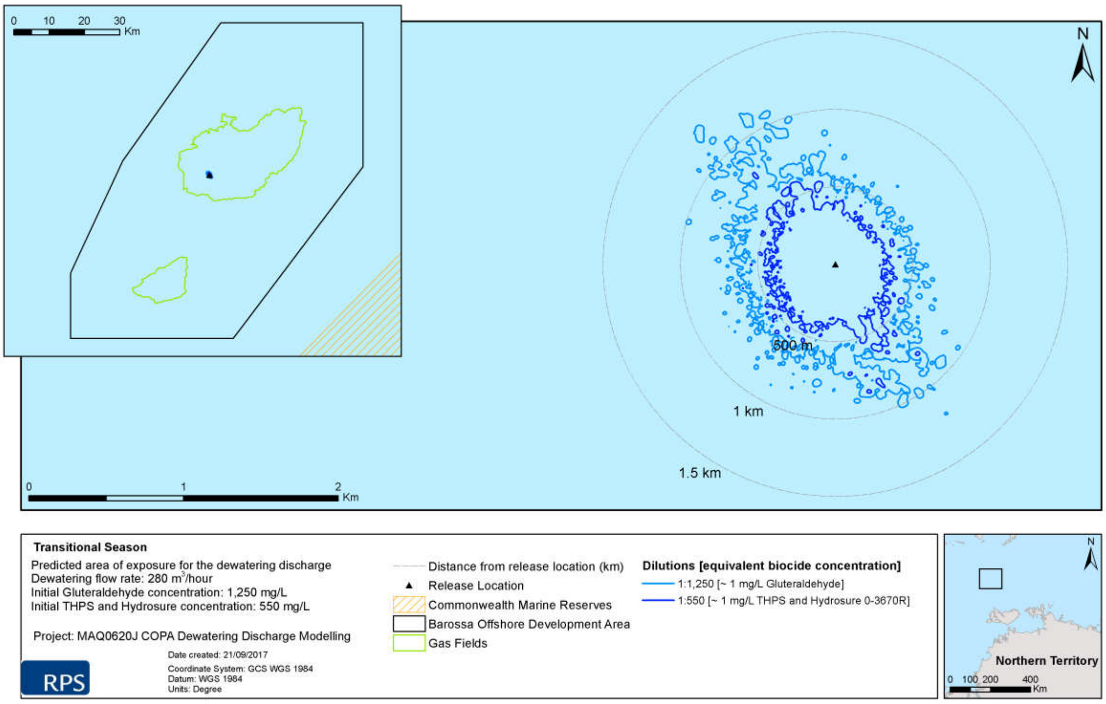

Figure 3.7 Predicted extent to achieve dilutions resulting in biocide concentrations of 1 mg/L under transitional (March and September to November) conditions for the 280 m^3/h flow rate (96,710 m^3 total discharge).

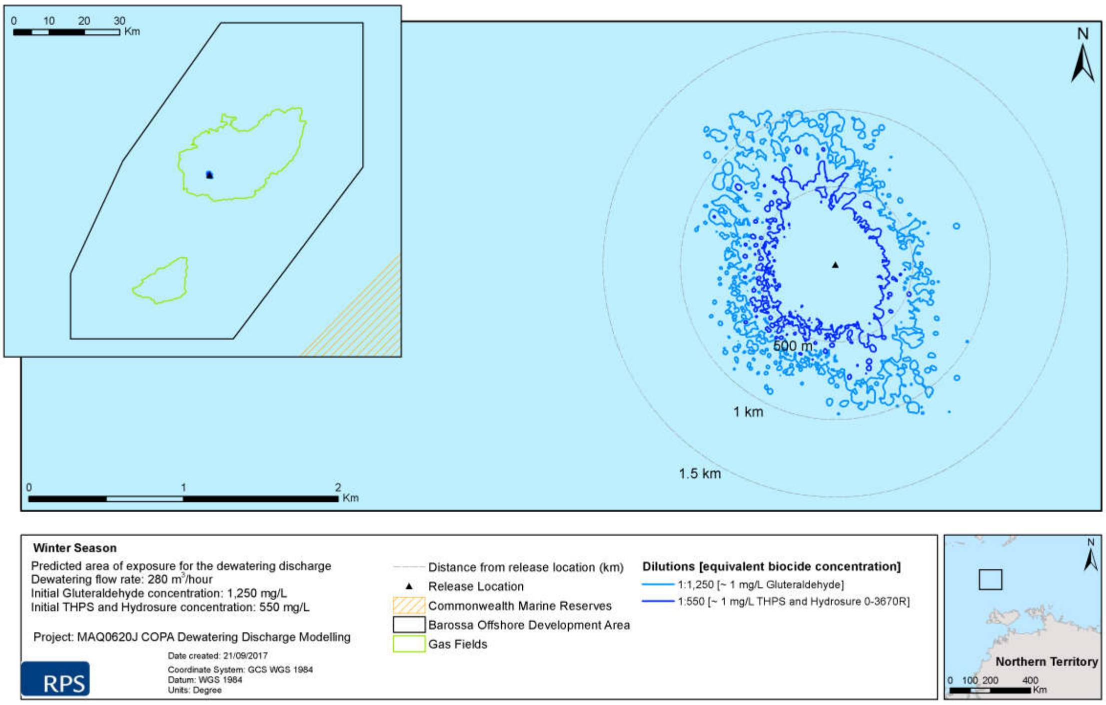

Figure 3.8 Predicted extent to achieve dilutions resulting in biocide concentrations of 1 mg/L under winter (April to August) conditions for the 280 m^3/h flow rate (96,710 m^3 total discharge).

3.2.3 Combined analysis

The far-field results demonstrated the dewatering discharge plume drifted horizontally through the water column in all directions from the release locations, whilst maintaining a low profile immediately above the seafloor. The maximum distances necessary to achieve dilutions equivalent to 1 mg/L were predicted to occur northwest and southeast of the release location (i.e. the dewater discharge plume persisted northwest and southeast of the release location the greatest distances before reaching the required dilutions of 1:1,250 for Glutaraldehyde and 1:550 for THPS or Hydrosure 0-3670R, respectively).Table 3.3 provides a summary of the area of coverage and maximum distance achieve dilutions resulting in biocide concentrations of 1 mg/L, once all of the model results have been overlaid for 2010, 2012 and 2014 conditions (for all seasons).

The combined predicted area of coverage was 1.14 km^2 based on the use of Glutaraldehyde biocide and 0.75 km^2 for either THPS or Hydrosure 0-3670R biocide. The maximum distance predicted was 1.27 km based on the use of Glutaraldehyde biocide.

Figure 3.9 show the extent to achieve dilutions resulting in biocide concentrations of 1 mg/L based on the seasonally combined model results (including all 2010, 2012 and 2014 conditions). Note that the images represent the lowest predicted dilution at any given time-step through the water column and do not take into account frequency or duration.

Table 3.3 Summary of the area of coverage and maximum distance to achieve dilutions resulting in biocide concentrations of 1 mg/L.

Biocide	Initial biocide concentration (mg/L)	Dilution required to achieve biocide concentrations of 1 mg/L	Area of coverage (km^2)	Maximum distance (km) from the release location
Gluteraldehyde	1,250	1:1,250	1.14	1.27
THPS and Hydrosure 0-3670R	550	1:550	0.75	0.92

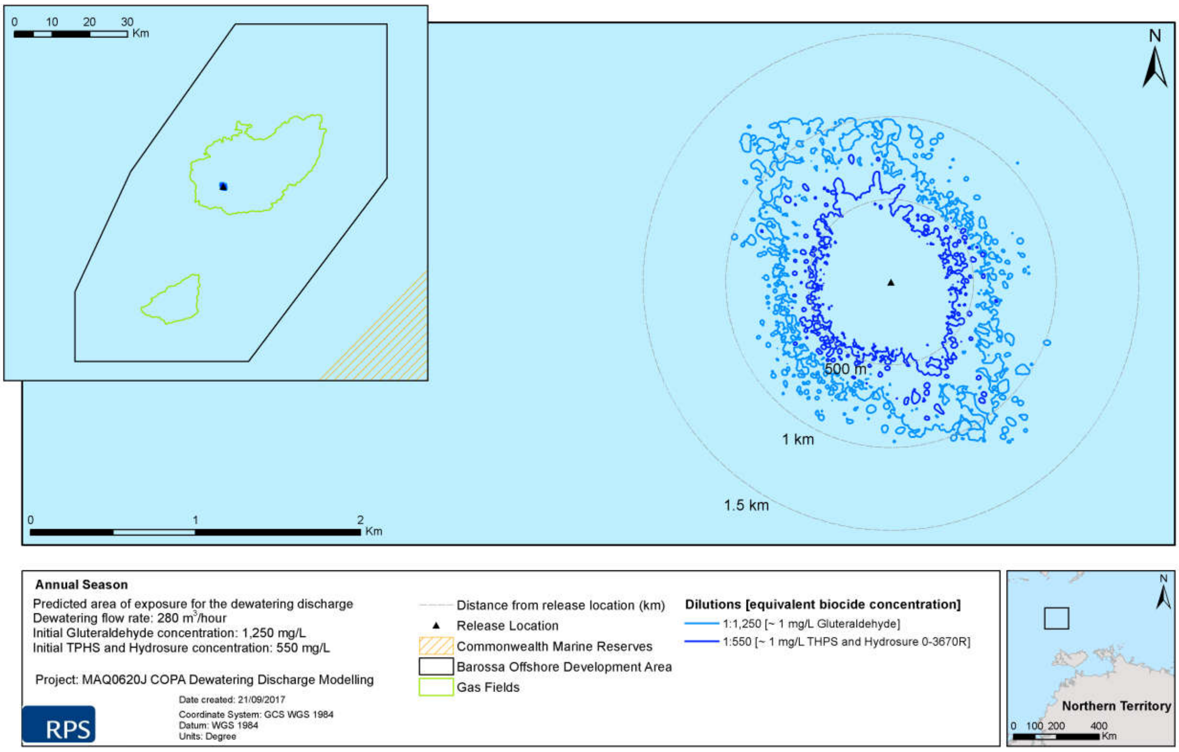

Figure 3.9 Predicted extent to achieve dilutions resulting in biocide concentrations of 1 mg/L any time of year (January to December) for the 280 m^3/h flow rate (96,710 m^3 total discharge).

4.0 References

Andersen, O.B. 1995. 'Global ocean tides from ERS 1 and TOPEX/POSEIDON altimetry'. Journal of Geophysical Research: Oceans, vol. 100, no. C12, pp. 25249–25259.

Baumgartner, D., Frick, W. and Roberts, P. 1994. Dilution models for Effluent Discharges, U.S. Environment Protection Agency, Newport.

Brandsma, M.G. and Sauer Jr, T.C. 1983a. 'The OOC Model: Prediction of Short Term fate of Drilling fluid in the Ocean. Part 1: Model Description'. Proceedings of MMS Workshop on An Evaluation of Effluent Dispersion and Fate Models for OCS Platforms. Minerals Management Service, Santa Barbara, California, pp. 58–84.

Brandsma, M.G. and Sauer Jr, T.C. 1983b. 'The OOC Model: Prediction of Short Term fate of Drilling fluid in the Ocean. Part 2: Model Results'. Proceedings of MMS Workshop on An Evaluation of Effluent Dispersion and Fate Models for OCS Platforms. Minerals Management Service, Santa Barbara, California, pp. 86-106.

Burns, K., Codi, S., Furnas, M., Heggie, D., Holdway, D., King, B. and McAllister, F. 1999. 'Dispersion and Fate of Produced Formation Water Constituents in an Australian Northwest Shelf Shallow Water Ecosystem'. Marine Pollution Bulletin, vol. 38, no. 7, pp. 593–603.

Chassignet, E.P., Hurlburt, H.E., Smedstad, O.M., Halliwell, G.R., Hogan, P.J., Wallcraft, A.J., Baraille, R. and Bleck, R. 2007. 'The HYCOM (Hybrid Coordinate Ocean Model) data assimilative system'. Journal of Marine Systems, vol. 65, no. 1, pp. 60–83.

Chassignet, E., Hurlburt, H., Metzger, E., Smedstad, O., Cummings, J and Halliwell, G. 2009. 'U.S. GODAE: Global Ocean Prediction with the HYbrid Coordinate Ocean Model (HYCOM)'. Oceanography, vol. 22, no. 2, pp. 64–75.

Chevron Australia Pty Ltd (Chevron). 2015, Wheatstone Project: Offshore Facilities and Produced Formation Water Discharge Management Plan: Stage 1. Document No: WS0-0000-HES-PLN-CVX-000-00101-000, Chevron.

Davies, A.M. 1977a. 'The numerical solutions of the three-dimensional hydrodynamic equations using a B-spline representation of the vertical current profile'. In: Nihoul, J.C. (ed). Bottom Turbulence: Proceedings of the 8th Liège Colloquium on Ocean Hydrodynamics, Elsevier Scientific, Amsterdam, pp. 1–25.

Davies, A.M. 1977b. 'Three-dimensional model with depth-varying eddy viscosity'. In: Nihoul, J.C. (ed), Bottom Turbulence: Proceedings of the 8th Liège Colloquium on Ocean Hydrodynamics, Elsevier Scientific, Amsterdam, pp. 27–48.

Frick, W.E., Roberts, P.J.W., Davis, L.R., Keyes, J., Baumgartner, D.J. and George, K.P. 2003. Dilution Models for Effluent Discharges (Visual Plumes) 4th Edition. Ecosystems Research Division U.S. Environmental Protection Agency, Georgia.

Fugro. 2015. Barossa Field Meteorological, Current Profile, Wave and CTD Measurements – Final Report. Reporting Period: 8 July 2014 to 16 July 2015. Unpublished report prepared for ConocoPhillips Australia Pty Ltd., Perth, Western Australia.

G-Biosciences. 2017. Safety Data Sheets. https://www.gbiosciences.com/image/pdfs/msds/786-1045_msds.pdf

Gordon, R. 1982. 'Wind driven circulation in Narragansett Bay' PhD thesis. Department of Ocean Engineering, University of Rhode Island.

Isaji, T. and Spaulding, M. 1984. 'A model of the tidally induced residual circulation in the Gulf of Maine and Georges Bank'. Journal of Physical Oceanography, vol. 14, no. 6, pp. 1119–1126.

Isaji, T., Howlett, E., Dalton C., and Anderson, E. 2001. 'Stepwise-continuous-variable-rectangular grid hydrodynamics model', Proceedings of the 24th Arctic and Marine Oil Spill Program (AMOP) Technical Seminar (including 18th TSOCS and 3rd PHYTO). Environment Canada, Edmonton, pp. 597–610.

Khondaker, A.N. 2000. 'Modeling the fate of drilling waste in marine environment – an overview'. Journal of Computers and Geosciences, vol. 26, no. 5, pp. 531–540.

King, B. and McAllister, F.A. 1997. 'The Application of MUDMAP to Investigate the Dilution and Mixing of the Above Water Discharge at the 'Harriet A' Petroleum Platform on the Northwest Shelf'. In: Modelling the Dispersion of Produced Water Discharge in Australia, Canberra, Australian Capital Territory.

King, B. and McAllister, F.A. 1998. 'Modelling the dispersion of produced water discharges', APPEA Journal, pp. 681–691.

Koh, R.C.Y. and Chang, Y.C. 1973. Mathematical model for barged ocean disposal of waste. United States Environmental Protection Agency, Washington.

Kostianoy, A.G., Ginzburg, A.I., Lebedev, S.A., Frankignoulle, M. and Delille, B. 2003. 'Fronts and mesoscale variability in the southern Indian Ocean as inferred from the TOPEX/POSEIDON and ERS-2 Altimetry data'. Oceanology, vol. 43, no. 5, pp. 632–642.

Ludicone, D., Santoleri, R., Marullo, S. and Gerosa, P. 1998. 'Sea level variability and surface eddy statistics in the Mediterranean Sea from TOPEX/POSEIDON data. Journal of Geophysical Research, vol. 103, no. C2, pp. 2995–3011.

Matsumoto, K., Takanezawa, T. and Ooe, M. 2000. 'Ocean tide models developed by assimilating TOPEX/POSEIDON altimeter data into hydrodynamical model: A global model and a regional model around Japan'. Journal of Oceanography, vol. 56, no.5, pp. 567–581.

Owen, A. 1980. 'A three-dimensional model of the Bristol Channel'. Journal of Physical Oceanography, vol. 10, no. 8, pp. 1290–1302.

Philander, S.G. 1990. El Niño, La Niña, and the Southern Oscillation. Academic Press, San Diego.

Rasmusson, E.M. and Wallace, J.M. 1983. 'Meteorological aspects of the El Niño/southern oscillation'. Science, vol. 222, no. 4629, pp. 1195–1202.

Roberts, P & Tian, X 2004, 'New experimental techniques for validation of marine discharge models', *Environmental Modelling and Software*, vol. 19, no. 7, pp. 691–699.

Spaulding, M.L., Kolluru, V.S., Anderson, E. and Howlett, E. 1994. 'Application of three-dimensional oil spill model (WOSM/OILMAP) to hindcast the Braer Spill'. Spill Science and Technology Bulletin, vol. 1, no. 1, pp. 23–35.

Yaremchuk, M. and Tangdong, Q. 2004. 'Seasonal variability of the large-scale currents near the coast of the Philippines'. Journal of Physical Oceanography, vol. 34, no., 4, pp. 844–855.

Qiu, B. and Chen, S. 2010. 'Eddy-mean flow interaction in the decadally modulating Kuroshio Extension system'. Deep-Sea Research II, vol. 57, no. 13, 1098–1110.

Zigic, S., Zapata, M., Isaji,T., King, B. and Lemckert, C. 2003. 'Modelling of Moreton Bay using an ocean/coastal circulation model'. Proceedings of the 16th Australasian Coastal and Ocean Engineering Conference, the 9th Australasian Port and Harbour Conference and the Annual New Zealand Coastal Society Conference, Institution of Engineers Australia, Auckland, paper 170.